Brain mapping of auditory hallucinations and illusions induced by direct intracortical electrical stimulation

Chloé Jaroszynski, Ricardo Amorim-Leite, Pierre Deman, Marcela Perrone-Bertolotti, Florian Chabert, Anne-Sophie Job-Chapron, Lorella Minotti, Dominique Hoffmann, Olivier David, Philippe Kahane

Brain Stimulation 15 (2022) 1077–1087

Contents lists available at ScienceDirect

Brain Stimulation

journal homepage: http://www.journals.elsevier.com/brain-stimulation

Brain mapping of auditory hallucinations and illusions induced by direct intracortical electrical stimulation

Chloé Jaroszynski [a, *], Ricardo Amorim-Leite [a], Pierre Deman [a], Marcela Perrone-Bertolotti [b], Florian Chabert [a], Anne-Sophie Job-Chapron [a], Lorella Minotti [a], Dominique Hoffmann [a], Olivier David [a, c, **, 1], Philippe Kahane [a, ***, 1]

[a] Univ. Grenoble Alpes, CHU Grenoble Alpes, Inserm, U1216, Grenoble Institut Neurosciences, GIN, 38000, Grenoble, France
[b] Univ. Grenoble Alpes, CNRS, UMR5105, Laboratoire Psychologie et NeuroCognition, LPNC, 38000, Grenoble, France
[c] Aix Marseille Univ, Inserm, INS, Institut de Neurosciences des Systèmes, Marseille, France

ARTICLE INFO

Article history:
Received 2 March 2022
Received in revised form
28 July 2022
Accepted 3 August 2022
Available online 8 August 2022

Keywords:
Auditory hallucination and illusion
Stereo-electroencephalography
Direct electrical stimulation
Gamma band activity
Probabilistic brain mapping

ABSTRACT

Background: The exact architecture of the human auditory cortex remains a subject of debate, with discrepancies between functional and microstructural studies. In a hierarchical framework for sensory perception, simple sound perception is expected to take place in the primary auditory cortex, while the processing of complex, or more integrated perceptions is proposed to rely on associative and higher-order cortices.

Objectives: We hypothesize that auditory symptoms induced by direct electrical stimulation (DES) offer a window into the architecture of the brain networks involved in auditory hallucinations and illusions. The intracranial recordings of these evoked perceptions of varying levels of integration provide the evidence to discuss the theoretical model.

Methods: We analyzed SEEG recordings from 50 epileptic patients presenting auditory symptoms induced by DES. First, using the Juelich cytoarchitectonic parcellation, we quantified which regions induced auditory symptoms when stimulated (ROI approach). Then, for each evoked auditory symptom type (illusion or hallucination), we mapped the cortical networks showing concurrent high-frequency activity modulation (HFA approach).

Results: Although on average, illusions were found more laterally and hallucinations more posteromedially in the temporal lobe, both perceptions were elicited in all levels of the sensory hierarchy, with mixed responses found in the overlap. The spatial range was larger for illusions, both in the ROI and HFA approaches. The limbic system was specific to the hallucinations network, and the inferior parietal lobule was specific to the illusions network.

Discussion: Our results confirm a network-based organization underlying conscious sound perception, for both simple and complex components. While symptom localization is interesting from an epilepsy semiology perspective, the hallucination-specific modulation of the limbic system is particularly relevant to tinnitus and schizophrenia.

1. Introduction

Conscious experience, whether in health or disease, stems from the integration of cortical signals originating from a complex landscape of spatially distinct yet temporally synchronized brain regions [1]. At the interface with the environment and the sensory organs, highly specific primary cortices have been proposed to occupy the ground level of a hierarchical perceptual architecture [2]. In this framework, the incoming sensory signal is fed forward with growing levels of integration but decreasing specificity to the

* Corresponding author.
** Corresponding author. Univ. Grenoble Alpes, CHU Grenoble Alpes, Inserm, U1216, Grenoble Institut Neurosciences, GIN, 38000, Grenoble, France.
*** Corresponding author.
E-mail addresses: chloe.jaroszynski@univ-grenoble-alpes.fr (C. Jaroszynski), olivier.david@inserm.fr (O. David), philippe.kahane@univ-grenoble-alpes.fr (P. Kahane).
[1] Co-last authors.

https://doi.org/10.1016/j.brs.2022.08.002

higher order regions of this hierarchy, in order for perception and cognitive processes to take place [3]. In the auditory modality, one therefore expects original sound perceptions to be first encoded in the posterior superior temporal gyrus, and modulations to be encoded in secondary, associative, or integrative areas, such as in the ventral and dorsal auditory streams and the insula [4]. [5].

In epilepsy, conscious perceptions may originate not from peripheral sensory information but from neural discharges during seizure activity, directly in the brain regions usually responsible for these perceptions [6,7]. Thus, the patient's experience of seizures, or semiology, which initially guides the evaluation and hypothesis on the possible location of the epileptogenic region [8], also informs on the cortical localizations and interactions resulting in perception. In particular, auditory auras found in 1.3–2.4% of focal epileptic seizures [9,10], have mainly been linked to seizure onset zones located in the auditory cortex at the posterior portion of the superior temporal gyrus, including Heschl's gyrus and the auditory association cortex, as well as in parietal or frontal regions.

Furthermore, DES has proven a good proxy to study brain function and organisation outside of epileptic seizures, allowing to map functionally eloquent areas during the clinical work-up prior to surgery. Past studies using DES have shown that repeated stimulation of the same brain region did not consistently produce the same effect, and conversely, stimulation of widely distributed areas of the brain could yield similar symptoms [5]. These elements argue in favor of a distributed network of interconnected and synchronized neurons underlying perception and cognitive function, but the way this network is organized remains an open question.

With the present study, we thus aim at better characterizing the cortical networks underlying DES-induced auditory hallucinations and illusions in a large cohort of 50 epileptic patients who underwent stereotactic intracerebral EEG (SEEG) recordings as part of their presurgical evaluation. We used DES to interrogate the influence of the type of perception on the cortical networks involved, with on one hand hallucinations occurring sine *materia,* or despite no external corresponding sound source, and on the other hand illusions consisting in an abnormal modulation of an existing sensory input.

First, in a Region Of Interest – ROI – approach, we related the observed symptoms to the stimulation site. We hypothesized that both illusions and hallucinations would be evoked from auditory regions. However, owing to the hierarchical framework for sensory perception, we expected to find hallucinations mainly elicited in the primary auditory cortex [5] (regions TE1.0, 1.1 and 1.2 in Juelich's atlas), while the modulatory component specific to illusions was expected to be triggered by stimulation to secondary associative or higher order auditory regions of the temporal lobe, or even regions of the ventral and dorsal auditory streams [6]. In addition, we expected to find no primary auditory sites to elicit illusions.

Then, we performed probabilistic mapping of high frequency activities (HFA, 70–150 Hz) elicited locally and at distant sites during stimulation, when auditory symptoms were produced, to establish the link between the observed symptoms and the cortical network disturbed by the stimulation procedure. From a methodological standpoint we hypothesized that the cortical modulations observed during stimulation are representative of the subsequent perceptual consequence. By confining to the time window defined by the stimulation, and with appropriate management of the stimulation artifact, results will thus be free of post-discharge related biases.

From a symptom mapping point of view, we expect for both phenomena to be linked to networks of auditory processing, involving the superior temporal lobe from its posterior primary auditory cortex, to its anterior semantic processing related regions, as well as the fronto-parietal regions of the motor integration. We also expect the limbic system, with the insula, hippocampus, amygdala, and cingulate cortex [11], to play a significant role in the involved networks, particularly given that both illusions and hallucinations diverge from the normal sensory representations. There are two aspects of the limbic system that seem particularly relevant. First, the perception of abnormal sounds, identified as not originating from the normal environment, is likely to bear an abnormal emotional valence, which would be determined in particular in the anterior insula and amygdala. The second aspect relates to the gating mechanisms mediated by auditory limbic connections, which have been extensively studied in the context of tinnitus [12–15], a phantom sound perception which would belong to the hallucination category as defined in the present study.

2. Materials and methods

2.1. Participants

A total of 109 patients presenting focal drug resistant epilepsy found eligible for surgery underwent standard pre-surgical evaluations using intracerebral recordings at Grenoble-Alpes University Hospital. All patients gave written informed consent to carry out SEEG exploration as well as non-invasive examinations including high resolution magnetic resonance (MRI) imaging, video-EEG monitoring, neuropsychological assessment, and computed tomography (CT) scanning. For the purpose of this study, we reviewed the results of all DES procedures performed over the period of time, following standardized procedures used at the hospital [16]. We identified 50 patients who experienced auditory symptoms during SEEG evaluation, with the electrically induced auditory symptoms unrelated to normal seizure symptoms (patient characteristics are documented in supplementary material: Table 1).

2.2. Electrode implantation and localization

Cortical implantation selection was entirely based on clinical purposes, with no reference to the present experimental protocol. Eleven to fifteen semi-rigid, multi-lead electrodes were stereotactically implanted in each patient (stereotactic EEG –SEEG-) [17,18] using a robot-assisted technique [19]. The SEEG electrodes had a diameter of 0.8 mm and, depending on the target structure, consisted of 8–15 contact leads 2 mm wide and 1.5 mm apart (i.e. 3.5 mm center-to-center, DIXI Medical Instruments). Implantation was unilateral in 35 cases (11 right-sided, 24 left-sided) and bilateral in 16 cases. Patients underwent a preoperative MRI scan and a postoperative MRI or CT scan. Preoperative and postoperative scans were co-registered in order to obtain electrode position coordinates in subject space. Transform to standard space was computed using SPM12 (Statistical Parametric Mapping 12, Wellcome Department of Imaging Neuroscience, University College London, www.fil.ion.ucl.ac.uk/spm), and electrode positions were then expressed in MNI coordinates. Visual inspection for all electrode locations was performed, to check for correct co-registration and to detect whether contacts were in grey or white matter. Neuroanatomical labelling of MNI coordinates of electrode contacts was performed using an in-house software, IntrAnat Electrodes [20]. The Juelich Brain atlas parcellation scheme was chosen to define the regions of interest of the present study for its high precision, based on post-mortem cytoarchitectonic analysis, in the peri-auditory regions [21,22].

2.3. SEEG recordings and stimulations

2.3.1. Experimental setup

SEEG recordings lasted from 1 to 3 weeks. A Micromed audio-video-EEG monitoring system was used to carry out experiments

Table 1
Synthesis and classification of des-evoked symptoms examined in the present study.

	All AS	Hallucinations			Illusions		Mixed		
		all	simple	complex	HS + HC		all	HS + I	HC + I
	n = 131	n = 57	n = 42	n = 12	n = 1	n = 64	n = 10	8	2
DCS side: Right/Left Hemisphere	53/77	19/36	12/31	5/6	0/0	28/35	5/5	3/5	1/0
Mean DES intensity (1–3 mA)	1,49	1,44	1,60	1,52	3	1,54	1,40	1,50	1,00
Mean DES duration (1–6 s)	4,04	3,88	3,88	4,58	3	4,19	5,00	4,63	6,50
AS lateralization									
Contralateral to the DES site	57	30	24	5	1	25	2	1	1
Ipsilateral to the DES site	4	3	3			1			
Bilateral	70	24	17	7		38	8	7	1
Associated signs									
none	105	47	37	10		49	9	8	1
somato-sensory/visual	7/2	4/0	3/0		1/0	3/2			
vestibular/vegetative	4/1	1/1	1/0	0/1		3/0			
facial flushing/feeling of warmth	1/2	0/2	0/2			1/0			
strangeness (environment)/feeling lost	1/1					1/1			
cephalic sensation/auditory déjà-vu	1/1	0/1		0/1		1/0			
akinesia/tonic motor/aphasia	1/1/5	0/1/2	0/1/2			1/0/3			
DCS sites									
Perirhinal cortex - BA36	2	1		1		1			
Temporal pole - BA38	1					1			
STG - BA22 (anterior part)	6	3	2		1	2	1	1	
STG - BA22 (posterior part)	7	3	2	1		3	1	1	
STG - BA22/42	12	3	3			7	2	1	1
STG - BA52	3	1	1			2			
STG - BA52/41	2					2			
TTG - BA41	27	13	13	1		12	2	1	1
TTG (BA41/42)	1	1	1						
TTG - BA42	15	7	7			7	1	1	
TTG - WM	2	2	2						
STS - BA22 (anterior part)	4	2		2		2			
STS - BA22 (posterior part)	1	1		1					
STS - BA22/21 (anterior part)	2	1		1		1			
STS - BA22/21 (posterior part)	2	1		1		1			
STS - posterior part (BA21)	1	1	1						
STS - BA22/21 (posterior part)	3	1		1		2			
STS - BA21 (anterior part)	1					1			
MTG - anterior part (BA21)	2					2			
MTG - posterior part (BA37)	1					1			
Insula - anterior part	2	2	2						
Insula - posterior part	14	9	6	3		4	1	1	
IPL (BA39/40)	5	2	2			3			
IPL (BA40)	2					2			
IPL (WM)	1					1			
posterior cingulate gyrus (BA23)	1						1	1	
posterior cingulate gyrus (BA31)	1					1			
OFC (BA11/12)	2					2			
IFG (BA44)	4	1	1			3			
IFG (WM)	1					1			
Mean latency (0–16 s)	2,86	2,61	2,48	3,25	6	3,19	2,20	2,00	3,00
Bilateral AS ipsiL > contraL	1					1			
Bilateral AS contraL > IpsiL	6					4	2	1	1
Bilateral AS non predominance	57	14	7	7		37	6	6	
high pitched noise/low pitched noise	9/5	7/4	7/4				2/1	2/1	
whistling/buzzing/sizzling	9/10/4	7/8/3	6/8/3		1/0/0		2/2/1	2/2/1	
whooshing/whirring sound	3/3	3/3	3/3						
other sound	9	9	9						
song, music/speaking voices	3/4	3/4	1/0	2/3	0/1				
noise evoking a specific animal/object	1/5	1/4		1/4			1/1		1/1
other HC	1	1		1					
clogged ear	15					13	2	2	
clogged ear + resonance	4					4			
clogged ear + echo	1					1			
decreased intensity/increased intensity	6/6					6/5	0/1	0/1	
decreased tonality/increased tonality	5/2					4/0	1/2	1/1	0/1
decreased intensity + tonality	1					1			
echo	25					22	3	2	1
echo + decreased intensity	2					2			
echo + decreased tonality	1					1			
echo + increased tonality	5					4	1	1	
echo + delayed perception	1					1			
resonance/delayed perception/other	4/2/2					4/2/2			
delayed perception + resonance	1					1			

(Micromed, Treviso, Italy) offering up to 128 recording contacts, with a sampling frequency of 512 Hz, and acquisition bandpass filter between 0.1 and 200 Hz. Acquisition was performed using a referential montage with the reference electrode located in the white matter and all other recording sites in the grey matter. For signal analysis, a bipolar montage between adjacent contacts of the same electrode was used, to improve sensitivity to local current generators.

DES was typically performed in 1 to 3-h sessions over multiple days under continuous video-EEG monitoring, to reproduce the patient's habitual clinical seizures and to map functionally relevant areas to be spared during surgery. DES was applied between two adjacent electrode contacts (bipolar stimulus) using a current generator delivering alternative square wave pulses (Micromed, Treviso, Italy), and according to parameters known to produce no structural damage [23]. Following standard clinical procedure [16], DES was performed at 1 Hz (pulse width: 1 ms; DES duration: 40s) and at 50 Hz (pulse width: 0.5–1 ms; DES duration: 5s), with stepwise increasing intensities (0.5 to a maximum of 5 mA) until clinical responses were elicited (after-discharges or electro-clinical seizures).

The experimental setup allowed patients to be sitting upwards on the bed, facing the camera. Tasks typically included counting or listing series of words. Depending on the expected or observed clinical responses, other tasks could be undertaken (e.g., alternate forearm movements, finger tapping, listening to the observer's voice, picture naming, etc.). Patients were asked to report any symptom they experienced as soon as possible and were immediately examined and carefully questioned by the observer. Clinical and electrical findings were documented using a standardized form, and stored on hard drive.

2.3.2. DES-evoked auditory perceptions

DES-evoked auditory experiences occurring in the absence of any corresponding sound input were characterized as *hallucinations*, and further divided into *simple* hallucinations (elementary sounds such as clicking, whistling, ringing, buzzing) or *complex* hallucinations (elaborate auditory phenomena such as music or voices). In contrast, DES-induced modulations of existing environmental sounds were categorized as *illusions* (change in loudness, pitch, distortion, echo …). No additional sounds were presented to the participants other than the ambient sounds such as voices or environmental noises occurring in the room. DES-evoked perceptions bearing characteristics of both types were considered *mixed* responses (*i.e.,* echoing phenomenon accompanied by whistling sounds).

2.4. Data analysis

2.4.1. Review of iEEG recordings and pre-processing

The raw data for each DES trial inducing an auditory symptom at 50 Hz was reviewed and annotated. Because only three auditory symptoms were evoked using 1 Hz stimulations, those were not further analyzed for the present study.

Each trial was annotated as follows: 1) stimulation start and end (visually identified based on the stimulation artifact), 2) auditory symptom onset (based on the video recordings), and 3) end of the post-discharge (fast oscillations occurring due to stimulation). The post-discharge activity was identified by visual examination of the recordings by an expert neurologist. The primary post-discharge management strategy was to implement ROI and HFA modulation analyses in a target time window excluding post-discharge activity, which was the case during stimulation. The risk of the results being biased by post-discharge activity was therefore mitigated. Furthermore, among all the stimulations performed, 30% of recordings were found to present a post-discharge, and a total of 9 recordings with symptoms lasting longer than the duration of the stimulation. This thus provided insufficient data for robust HFA analysis in this selection of recordings to precisely map and compare whether results may have been influenced by subsequent post-discharges. In addition, the post-discharge activity in time-frequency domain is found to occupy the 3–45 frequency range, which was not the frequency range of interest in the present study. Finally, bad channels were automatically labeled and excluded from analysis [24].

2.4.2. ROI analysis

In this approach, the data was clustered by symptom type (i.e., illusion, hallucination, mixed). In case several auditory responses were obtained at different intensities for a given channel, only the response obtained at the lowest intensity was kept for analysis. To quantify the capacity of a given brain region to generate an auditory response upon stimulation, the responses from electrode contacts belonging to the same ROI were pooled together.

2.4.3. HFA analysis

To maximize the amount of data for robust network analysis, we kept all recordings during which a symptom was provoked using 50 Hz DES, irrespective of whether a symptom had previously been evoked at a lower intensity.

2.4.3.1. Single trial processing. First, single trials were processed following the epileptogenicity mapping procedure developed in our team [25] and recently used for language mapping [26]. Periods of interest of the SEEG recordings were taken during DES and baseline activity was chosen in the [30 5]s interval prior to stimulation onset (Fig. 1B). All time series were transformed into time-frequency maps for each channel (Fig. 1C). Spectral power was computed between 70 and 150 Hz with a 1 Hz frequency resolution, using a Hanning-tapered decomposition with a fixed window length of 1s and a 100 ms step size. A notch filter was applied to remove harmonics of line noise between 98 and 102 Hz, and between 148 and 152 Hz. Z-score normalization of DES time frequency maps was performed by dividing the DES signal to time frequency domain transform by the mean baseline estimate [27]. Stimulation artefacts suppressed by ignoring values of z-scored SEEG power above 10, and outliers were ignored by averaging over the frequency dimension when computing SEEG power timeseries. For sake of caution, SEEG power matrix elements with a z-value above 10 in over 5% of channels were removed, including those for which the threshold was not reached. The time frequency maps in the selected time bins were log-transformed and spatially interpolated to produce images for statistical analysis. In standard space, the power values for each electrode contact were mapped to the corresponding electrode contact position. Spatial interpolation restricted voxels to the structures most often explored in presurgical protocols for temporal lobe epilepsy, namely the neocortex, the hippocampus, and the amygdala. The method used is described in depth in Ref. [28]. Briefly, for each contact, mesh vertices within a 1 cm radius are detected and each vertex detected for at least one electrode is assigned the weighted average of the SEEG power values of all nearby electrodes, with weights chosen as the inverse of the distance between the vertex and the electrodes, the closest electrode thus receiving the highest weight. Gaussian smoothing was performed using a 3 mm kernel width, in the same order of magnitude as the distance between contacts, for family-wise error rate control in the case of spatially correlated imaging data [29].

A two-sample *t*-test was used to compare symptom perception to baseline and statistical significance was determined by the FWE-corrected associated p-value using $p < 0.05$ as a threshold. Thus, the

regions displaying significant HFA modulations during DES induced auditory symptoms were obtained for each trial.

2.4.3.2. Group level analysis. To specify the group average spatial distribution of recorded responses for each auditory symptom type evoked during DES, analysis ran as follows: first, a binary mask was derived from the SEEG log power statistical maps previously obtained at a $p = 0.05$ threshold (Fig. 1D). Voxels displaying significant SEEG power values during an auditory response were kept for further analysis and assigned to their corresponding atlas ROI. Each ROI containing at least one significant voxel was therefore considered active during the evoked symptom, while regions having received no significant voxel attribution were considered inactive. For visualization purposes, the atlas resolution was set at 3 mm isotropically and ROIs were dilated by one voxel to avoid gaps on surface-based representations.

ROI-level binary maps were averaged across trials to obtain group probability maps of symptom-related SEEG power modulation. For each symptom type, an additional threshold of minimum 10 recordings per ROI was applied for sake of reproducibility. The group probability maps, further referred to as HFA maps, range from 0 (no significant HFA power increase in the ROI during any of the recordings) to 1 (systematic HFA increase during symptom perception).

We determined the probability threshold to be used for statistical significance of the group level probability maps at a p-value <0.05 (henceforth referred to as alpha value to avoid confusion with the probability value) using surrogate distributions of group level probability for each ROI [30]. They were obtained by redistributing randomly in space the same number of activated ROIs at the single trial level and regenerating the group probabilities (for each condition and for the difference between condition). By doing this multiple times (19 realizations were done), we could generate null distributions of group probabilities under the assumption that spatial patterns were randomly distributed but with an equal degree of activation. This sets the probability threshold (at alpha<0.05) at a value specific to each ROI because of the heterogeneous spatial sampling between subjects.

3. Results

3.1. Initial assessment of recordings

A total number of 2610 cortical sites were recorded throughout the experiment, with 1578 sites in the right hemisphere and 1032 sites in the left hemisphere (Fig. 2A). A total number of 141 stimulations were reported to have elicited an AR during DES at 50 Hz and at intensities between 1 and 3 mA (mean 1.6 mA, median 1 mA). The median number of areas having elicited an auditory symptom per single patient was 2, and stimulation to different areas in the same patient was found to elicit different symptoms. Stimulations lasted between 0.5 s and 5 s (mean 4.1 s). Among the 141 associated recordings, 4 had all channels labeled as 'bad' and were not subsequently analyzed.

For ROI-based analysis, recordings of symptom evocation at lowest intensity were kept, narrowing down the analysis to 127 recordings and a corresponding number of auditory responses. For network analysis of symptom-related high frequency oscillation modulation, we chose to keep all good quality recordings to maximize the amount of data for the group analysis, so a total number of 137 recordings. With the components of mixed responses considered independently, there was a total count of 144 auditory symptoms for HFA analysis.

3.2. Overview of auditory responses to DES

Auditory responses (AR) were in majority the only sign reported upon stimulation (80% of cases), with a leftward preference (58.7% of AR evoked from the left hemisphere). The occasional co-occurring symptoms included aphasia, visual illusion, tachycardia, thermic sensations, tactile sensation or loss of sensation, vertigo, and drowsiness (Table 1). AR were perceived as bilateral in 70 cases and unilateral in 61 cases (46.5%). Among the unilateral AR, the majority (93%) were perceived on the contralateral side to the stimulation site.

A total number of 57 hallucinations were reported (43.5% of all AR). They were mainly simple hallucinations (73.7% of all hallucinations) consisting of elementary sounds, either continuous (such as whistling, buzzing, ringing, resonating, non specific noise), or impulsive (drum, hammer, clapping, ticking). Complex hallucinations involved more elaborate perceptions such as sounds reminding a specific object (washing machine, train, doorbell) or animal (fly, cicada), voices, or music (Table 1). In one case, the hallucination was a combination of complex and simple perceptions.

Participants reported an illusion in 56.5% of cases (Table 1), mainly in the form of an echo (34%), a sensation of clogged ears (20%), variations in sound intensity, amplitude, pitch, or lag. Combinations of illusions were also observed (25%).

Mixed responses were reported for 10 stimulations, a majority of which (80%) consisted of an illusion and a simple hallucination. In 2 cases a complex hallucination was coupled with an illusion.

3.3. ROI analysis

The distribution of the total implanted electrodes and the electrodes having elicited a given symptom is illustrated in Fig. 1. In the right hemisphere, we observed slightly more hallucinations (47%) than illusions (45%), and 6 mixed responses (7%). In the left hemisphere, illusions were predominant (60%) over hallucinations (32%) and mixed responses (7%). The covariance ellipses (Fig. 1. C) indicate the centers of mass of illusion and hallucination distributions and quantifies their level of dispersion and overlap in the three directions. Illusions showed greater dispersion and an antero-lateral shift compared to hallucinations, in both hemispheres but predominantly in the right. Hallucinations were located on average more postero-medially, with an orientation of the ellipse towards the temporal pole in the right hemisphere.

Responses were evoked from 42 cortical Juelich ROIs in both hemispheres, out of 248 atlas ROIs (Fig. 2B). Hallucinations covered 27 regions (18 ROIs of the left hemisphere, 9 ROIs of the right hemisphere), while illusions extended over 36 regions (18 ROIs in each hemisphere). Mixed responses were found in 7 regions (3 in the right hemisphere, 4 in the left).

Among these 42 regions, 21 were common to both hallucinations and illusions (Supplementary Table 2). They included auditory regions of primary (in Heschl's gyri: bilateral TE1.1, left TE1.0), secondary (bilateral TE2.2 in the planum temporale, right TE 2.1, and left temporo-insular region TeI), associative (TI of the left planum polare), and higher order processing (bilateral STS1; right STS2). They also included integrative regions of the posterior insula (bilateral Ig1, right Ig2), mid insula (left Id1), and IPL (left area PFcm and right area PFop). The proportion of hallucinations versus illusions was greater in the primary areas in the right hemisphere, but not in the left. The proportion of hallucinations was also greater in the left posterior and mid insula, the left secondary areas TeI and TE2.2. Conversely, illusions were predominant in the right secondary auditory area TE2.2 and higher order area STS2. In the left hemisphere, illusions were predominant in higher order and

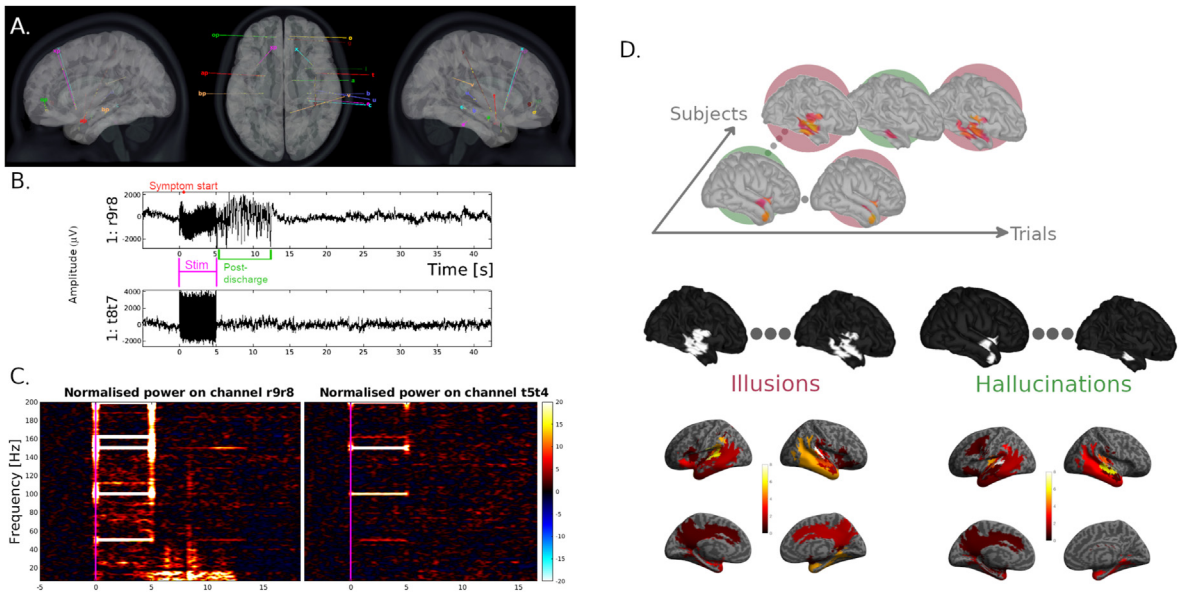

Fig. 1. Graphical representation of the processing pipeline. A. Electrode localization, after intra-subject coregistration and transformation to MNI space. According to their MNI coordinates, each contact is then paired with its correspond ROI from the Juelich parcellation scheme for ROI analysis. B. SEEG timeseries from 2 contacts, in the case of a 50 Hz stimulation. The symptom produced during this trial was a simple hallucination (buzzing sound). Stimulation lasted 5 s (between t = 0: DES ON and t = 5s: DES OFF). The auditory symptom started immediately after stimulation onset. The after-discharge ended at the PD mark, 8 s after stimulation cessation, as visible in the r9r8 channel, and not in the t5t4 channel. C. Time-frequency decomposition for the 2 channels after notch filtering and baseline normalization. The 50 Hz stimulation (bright horizontal lines) and its harmonics are visible, and the stimulation artifact is seen at the beginning and end of the stimulation (vertical lines). In channel t5-t4, no effect is observed during and after the end of the stimulation at any of the analyzed frequencies. Channel r9-r8 displays activity in the 80–140 Hz frequency band during the stimulation, and a low frequency activation corresponding to the post-discharge starting at the end of the stimulation. D. For HFA analysis, the SEEG power values are averaged for each channel and located at the corresponding MNI coordinates. A cortical map is produced for each participant and each trial using spatial interpolation of the sparse contact locations. The number of trials ranges from 1 to 8 per subject. The cortical maps are binarized, pooled together and clustered according to symptom type (hallucinations in green, illusions in red). The superposition of the binary maps yields the probability map, represented in example here, reflecting for all regions the likelyhood of having SEEG power modulation due to a given induced symptom. In the ROI analysis, the process is simpler: the binary maps are directly taken as the ROIs that elicited a symptom for each trial. The probabilistic maps represent the likelyhood that a given region may elicit a symptom if stimulated. (For interpretation of the references to color in this figure legend, the reader is referred to the Web version of this article.)

secondary auditory areas as well as in primary auditory area TE1.1 of Heschl's gyrus.

Several ROIs were exclusively involved in only one symptom type. Indeed, 6 hallucination-specific regions were found in the left hemisphere, including areas of the posterior insula (Ig2), hippocampus, frontal cortex, superior temporal sulcus, frontal operculum (OP6) and parietal operculum (OP2) were specific to hallucinations, but no regions of early auditory processing.

Illusion-specific regions ranged over a wider spatial extent, and included auditory regions of the superior temporal lobe. Primary auditory area TE 1.0 and higher order area TE3 were found in the left hemisphere, as well as mid insular, inferior parietal sulcus, and inferior frontal gyrus areas. In the right hemisphere, secondary and higher order auditory areas TE 2.1 and TE 3 were found, alongside mid, posterior and anterior insular regions, inferior parietal, inferior frontal, and orbitofrontal regions (Supplementary Table 3).

3.4. HFA analysis

In this approach, the recordings performed across over 2000 cortical sites were pooled together to perform probabilistic mapping of HFA modulations during AR. All regions represented in Fig. 3 showed significant modulation compared to baseline, with a minimum threshold of 10 recordings per ROI, as required for reproducibility purposes. Regions with high probability values were consistent in their HFA modulation with respect to symptom perception, while regions with low probability did not systematically show HFA modulation across trials during symptom perception. In addition, to control for variations in topography with an alpha-value of 0.05, a ROI-specific probability threshold was obtained to determine statistically significant results for each condition and to assess significant differences between the networks involved in hallucinations and illusions.

The total spatial coverage of HFA increase involved in hallucinations and illusions overlapped in 144 atlas regions bilaterally (out of N = 248), however only 31 common regions remained after statistical testing (alpha <0,05, see Supplementary Table S3 for detailed probability values). Both symptoms involved bilateral networks including primary, secondary, and associative auditory regions on the temporal lobe, as well as opercular, insular, parietal, and frontal regions (Fig. 3).

HFA modulations found significant for hallucinations only (Table 2a) ranged across 16 bilateral regions, including secondary auditory regions TE 2.1 bilaterally, as well as areas of periauditory – insular cortex, left area TI and right area TeI. Parietal opercular involvement was found specifically in the left hemisphere, inferior parietal sulcus in the right hemisphere, while bilateral frontal opercular areas were highlighted. In addition, left sensorimotor area 4a and right somatosensory area 3a were part of the hallucination-specific network, as well as higher order areas left frontal area 44 and left fronto-orbital cortex. Limbic area CA1 of the hippocampus was highlighted in the left hemisphere.

Looking at significant differences between DES-evoked symptoms where hallucinations had significantly higher probabilities than illusions, 7 regions of the left limbic system and 1 region of the right limbic system were highlighted (Table 2b) in addition to areas 3a and TeI.

HFA modulations found significant for illusions only (Table 3a) ranged across 27 bilateral regions, including right early auditory area 1.2, associative auditory areas left TeI and left STS2, and right

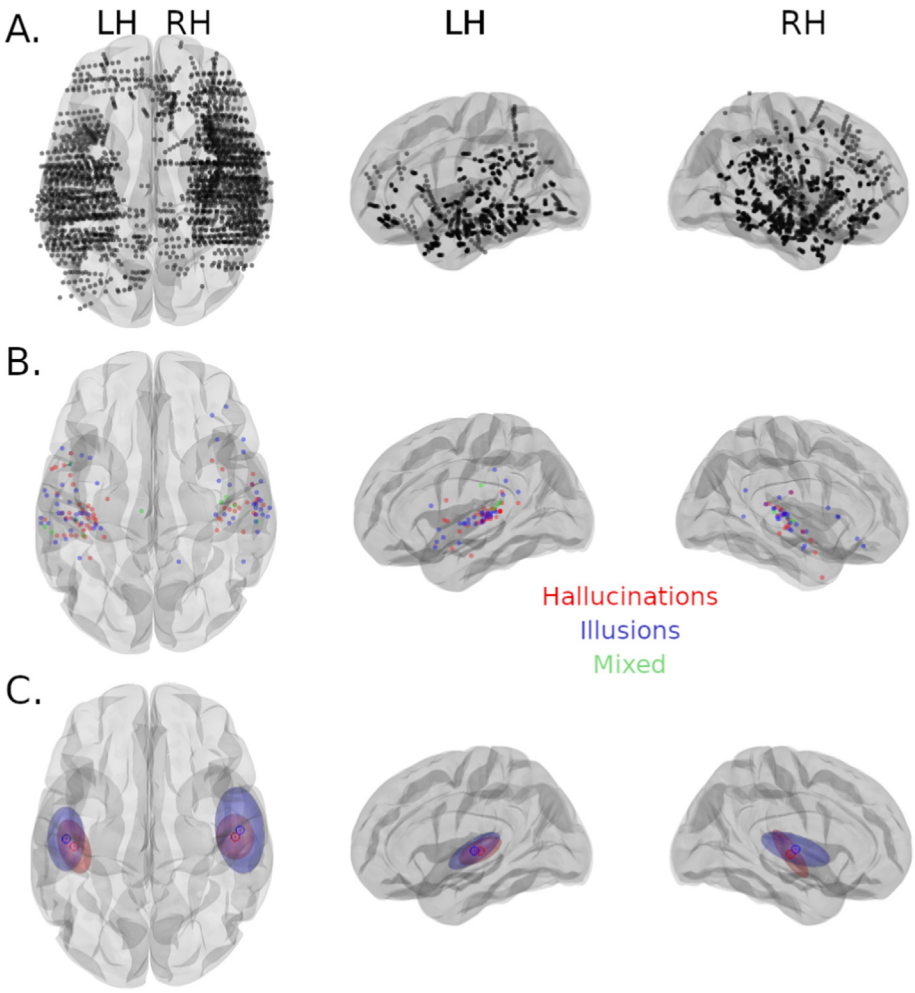

Fig. 2. Distribution of electrode contacts involved in the present study. A. Electrode contact location in MNI space for all recorded contacts during the span of the experiment. B. Distribution of the contacts having generated an auditory perception, per symptom type.C. 3D ellipsoid representation using mean and covariance of the contact distributions for hallucinations and illusions.

area TI. Specific insular involvement was found and included posterior, mid, and anterior areas bilaterally. The inferior parietal lobule was also involved bilaterally, while sensorimotor and somatosensory areas were highlighted in the right hemisphere. Higher order regions of the orbitofrontal cortex and inferior frontal cortex were also part of the illusion network.

Looking at significant differences between DES-evoked symptoms where illusions had significantly higher probabilities than hallucinations (Tables 3a and 3b), 6 regions of the left hemisphere were highlighted, including frontal opercular, fronto-orbital, anterior cingulate, and inferior parietal areas.

4. Discussion

The main findings of the present study were 1) illusions and hallucinations distribute differently in the brain but these distributions overlap to a large extent, with illusions more dispersed than hallucinations and more in the right hemisphere than in the left, 2) contrarily to what was expected, certain primary regions were found to evoke only illusions and certain higher order regions were found to evoke only hallucinations, 3) the probability maps of HFA power modulations span similarly far for each perception, however hallucinations involved a specific limbic network, while illusions involved a wider ranging specific fronto-parietal and insular network.

4.1. Does the auditory system match a hierarchical organisation of sensory cortices?

Our results shed a nuanced light on the hierarchical model proposed for sensory cortices, owing to the mix of perceptions induced at all levels of the proposed auditory architecture. Within this framework, DES of primary sensory areas is proposed to act as input at the initial perception level, and be fed forward as such to the next processing level in the hierarchy. In downstream processes, this signal is considered as an original perception, in other terms: a hallucination [31]. In the case of auditory perceptions, the characteristics of the hallucinations provoked by DES of the primary auditory cortex are defined depending on the precise location of the electrode contact, owing to the fine tonotopy and periodotopy of the primary auditory cortex [32–34]. On the other hand, stimulation of secondary sensory regions is expected to yield a different component of perception, with the stimulation not being recognized as initial input but as a piece of integrative information, thus an element of modulation of primary perception – an illusion [31]. In line with this model, illusions induced in our study were indeed found, in our ROI-analysis, specifically in regions of higher auditory, in multiple insular sites, in inferior parietal regions, and in the inferior frontal gyrus. In contrast however, no regions of the primary cortex were found exclusively evocative of hallucinations. Instead, the second part of the left posterior insula was specific to

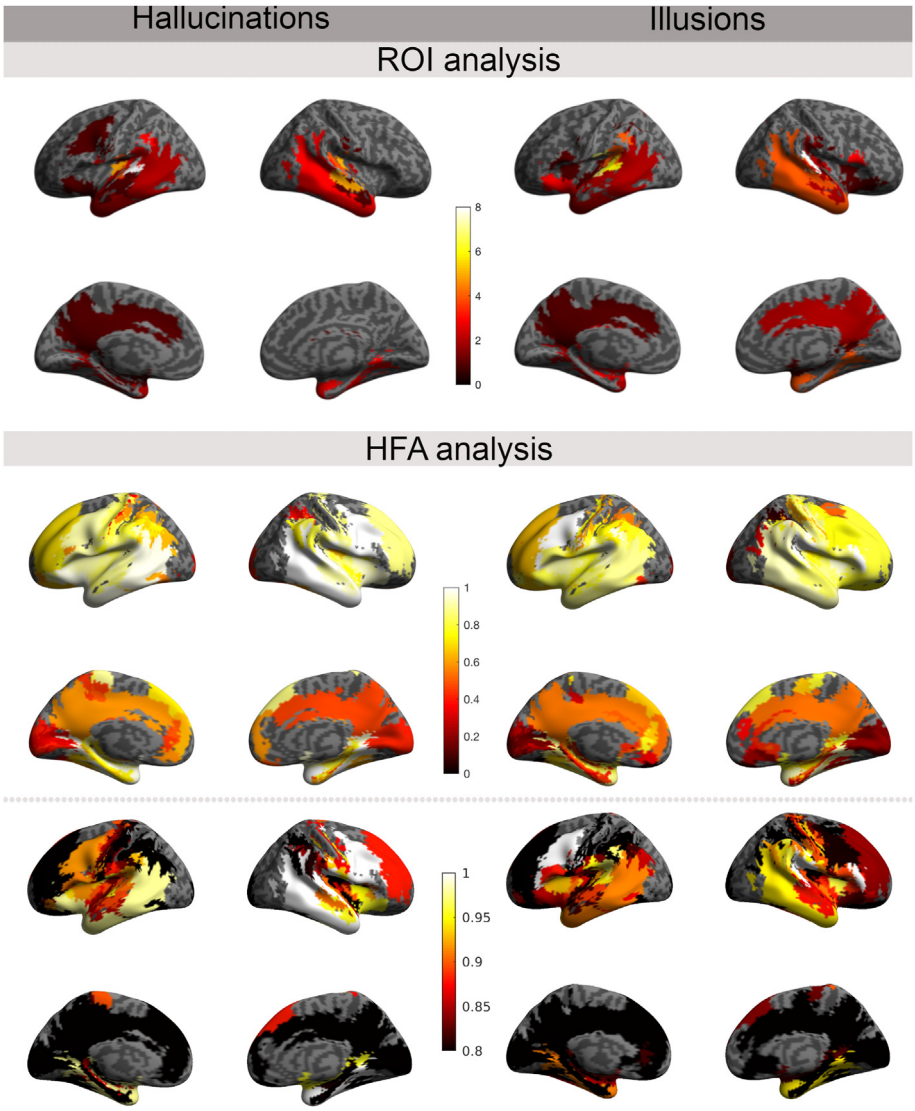

Fig. 3. Results of ROI and HFA analyses Top: results of the ROI analysis. Bottom: results of the HFA analysis, with a full (first line) and a thresholded (second line) colormap, to enhance differences between hallucinations and illusions.

Table 2a
Regions of the hallucination-specific HFA network (alpha <0.05). In bold are the regions where the difference between the probability maps for hallucinations and the probability maps for illusions was significant (p_hallucination − p_illusion is given in parentheses).

Hemisphere	Brain region	Jülich parcel	Probability
Left	Superior temporal gyrus	TE 2.1	0.95
		TI	0.87
	Parietal operculum	OP3	0.97
	Frontal operculum	OP6	0.92
	Orbito-frontal cortex	Fo7	0.92
	Pre-central gyrus	4a	0.89
	Inferior frontal gyrus	44	0.91
	Limbic - Hippocampus	CA1	0.87
Right	Sup. temporal gyrus	TE 2.1	1.00
		TeI	**0.95 (0.14)**
	Frontal Operculum	OP6	1.00
	Post-central gyrus	**3a**	**0.94 (0.23)**
	Inferior parietal sulcus	hIP 1	0.85
	Frontal-II (GapMap)	–	1.00
	Frontal-I (GapMap)	–	0.88
	Frontal-to-temp (GapMap)	–	0.96

hallucinations, as well as the secondary auditory area STS2. Furthermore, the left primary area TE 1.0, supposedly core auditory, related to illusions, not hallucinations. These results indicate that the primary auditory cortex is capable of higher order processing and that conversely, higher auditory areas such as the left STS2 of the ventral auditory processing stream and IPL of the dorsal processing stream, as well as posterior insular regions can be involved in early auditory processing, in line with previous suggestions of

Table 2b
Additionnal regions where the difference hallucination − illusion was significant.

Hemisphere	Brain region	Jülich parcel	Probability
Left	Hippocampus	CA2	0.75 (0.29)
		HC-presubiculum	0.70 (0.25)
		HC-transsubiculum	0.63 (0.27)
	Amygdala	IF	0.85 (0.37)
		SF	0.62 (0.31)
		CM	0.72 (0.49)
		VTM	0.63 (0.23)
Right	Hippocampus	HC-transsubiculum	0.77 (0.27)

Table 3a
Regions of the illusion-specific HFA network (alpha <0.05). In bold are the regions where the difference between the probability maps for illusions and the probability maps for hallucinations was significant (p_illusion − p_hallucination is given in parentheses).

Hemisphere	Brain region	Jülich parcel	Probability
Left	Sup. temporal gyrus	TE 3	0.84
		TeI	0.81
	Sup. temporal sulcus	STS2	0.82
	Frontal Operculum	**OP9**	**1.00 (0.24)**
		OP8	0.90
	Insula	Id2	0.94
		Id5	0.91
		Ia	0.89
		Ig2	0.86
	Inferior parietal lobule	**PGp**	**0.86 (0.21)**
		PFop	0.84
	Orbitofrontal cortex	**Fo4**	**0.88 (0.27)**
	Fusiform gyrus	**FG4**	**0.87 (0.23)**
	Inferior parietal sulcus	hIP 2	0.76
Right	Early auditory	TE 1.2	0.88
	Sup. temporal gyrus	TI	0.88
	Insula	Id3	0.91
		Id2	0.88
		Ia	0.88
		Id4	0.86
	Inferior frontal gyrus	45	1.00
	Inferior parietal lobule	Pfm	0.96
		PF	0.92
		PGa	0.92
		PFt	0.91
	Pre-central gyrus	4p	0.93
	Post-central gyrus	3b	0.90

non-core auditory areas presenting sensitivity to acoustic features of sound [34–36]. This fuels the debate on the precise organization of auditory processing in humans: the parallel with the core-belt-parabelt model described in non-human primates remains to be fully established [36]. High-resolution multimodal brain atlases do not fully align with the precise subdivisions obtained using cytoarchitectonic mapping techniques: in line with non-human primate literature, Glasser's atlas [37] depicts a medial belt region overlapping over primary regions Te1.0 and 1.2 in Juelich's atlas [22]. The existence of mixed responses, as well as previous evidence of different symptom types being evoked at the same electrode contact, may reflect how certain cortical assemblies act as gateways between the components of the sensory structure.

With the HFA analysis, the aim was to further contrast the network of regions involved in each perception, with modulations mirroring the emergence of conscious perception [38]. For both auditory phenomena, the involvement of auditory processing networks was expected, possibly ranging from the superior temporal lobe to fronto-parietal areas following dorsal and ventral streams, albeit with potential differences in extent. We also expected the involvement of the limbic system in the perception of sounds identified as deviating from the normal environment and possibly involving the activation of gating mechanisms mediated by auditory limbic connections.

The common, consistent involvement during illusions and hallucinations of opercular, insular, and inferior parietal lobule regions in addition to periauditory cortices indeed argues in favor of a widespread functional network underlying both perceptions. This is in line with previous findings on dorsal and ventral streams of auditory processing [39,40].

Table 3b
Additionnal regions where only the difference illusion − hallucination was significant.

Hemisphere	Brain region	Jülich parcel	Probability
Left	pACC	p24ab	0.82 (**0.36**)
	Inferior parietal lobule	PFm	0.79 (**0.11**)

The main differences were found in the distribution of probabilities in the HFA-modulated network overlap. Strikingly, hallucinations modulated the limbic system to a greater extent than illusions, which is in line with the two aspects of limbic involvement in auditory processing. Firstly, it may be that hallucinations, as the perception of a non existing sound, may bear a more salient emotional content than illusions, and this emotional content would be mediated by the amygdala and hippocampus. However, this remains speculative in the present study given that emotional valence of the perceptions was not assessed. Secondly, this finding is relevant with respect to the role of the limbic system in gating phantom perceptions, identified as deviating from the normal sensory environment. Interestingly, illusions were found to modulate the inferior parietal cortex more strongly than hallucinations. This region belongs to the dorsal auditory stream and is involved in localization of moving sound sources, which is coherent with the majority of illusions in the present study involving spatio-temporal features such as echoes and sound lag.

Interestingly, the insula was involved at the ROI level as well as in the HFA analysis. According to the ROI analysis, mainly the left posterior insula was a key region for evoking auditory hallucinations, while illusions were evoked bilaterally towards more anterior sections of the insula. The posterior insula is directly adjacent to the somatosensory and the auditory cortices, and has been described as the primary region of interoception, involved in a wide range of sensory perceptions, as well as in contemplative activities and fine motor behavior. The mid insula integrates the posterior multisensory components with vegetative cues and emotional load, and connects to the anterior insula. The anterior insula together with the anterior cingulate cortex, constitutes the main nodes of the saliency network, responsible for tuning in attention to relevant stimuli among the wealth of incoming sensations. Our ROI-analysis results thus agree with a differentiated role played by the insula depending on the level of complexity – or the degree of integration – of the perception. In line with this observation, in the networks analysis the mid or dysgranular insula was found bilaterally involved in the network common to illusions and hallucinations. In the symptom-specific networks, areas ranging across the entire insula were involved in illusions, arguing in favor of illusions requiring more integration than hallucinations, and of the insula being an integration channel with a gradient from posterior to anterior areas.

4.2. Relevance for pathological conditions

Intracortical exploration for severe epilepsy has a history of auditory signs mostly being elicited by stimulating the superior temporal gyrus (STG) or the middle temporal gyrus (MTG) [41,42], as well as the temporal pole [42,43], the mesio-temporal lobe [44–46], the temporo-occipital junction [42], the parietal lobe [41], and the insular cortex [47–49]. These elements, however, result from different stimulation approaches (intra-operative electrocorticography, extra-operative subdural or depth electrodes) with stimulation paradigms varying across series, and the exact locations of the stimulated contacts were often not provided. Furthermore, auditory symptoms have mainly been reported as a side-effect of studies targeting other brain processes [41–50]. The present study proposes a unified approach in a large cohort of participants to establish the value of auditory symptoms in semiology to guide the location of the epileptic zone.

The large amount of spatial overlap between the regions inducing each symptom type, the presence of illusions in primary regions and primary auditory perceptions in secondary or higher order areas, and finally, the presence of mixed responses, do not argue in favor of a strong localizing value of specific auditory signs based on their level of complexity in epileptic semiology. The lack of univoqual anatomical specificity of auditory symptoms rather illustrates how the emergence of ictal signs and symptoms depends not only on the initial location of the epileptic discharge but also on its spread, type, and the complex spatial-temporal interactions that it produces within a multiconnected brain network [6].

This study also presents a particular interest for auditory related pathologies. The auditory-limbic emotional processing and gating mechanisms are in line with previous findings regarding tinnitus, which qualifies as an auditory hallucination. In tinnitus, the perception itself and the associated distress and annoyance may be respectively facilitated by both auditory-limbic mechanisms [12,14]. Another result which is relevant specifically to tinnitus perception, and not its distress component, is the involvement of the parietal operculum and in particular OP2 in the ROI analysis and OP3 in the HFA analysis. These regions have been shown to participate in auditory-somatosensory integration, and have been proposed to mediate erroneous phantom sound perception following acoustic trauma [51,52].

In schizophrenia, hallucinations are a salient symptom, often loaded with negative emotion, however whereby tinnitus has been used as a basis of understanding [53]. Similarly, a lack of top-down auditory-limbic regulation to block out irrelevant or erroneous incoming sensory information has been suggested as facilitating the emergence of hallucinations [54]. However, the perceptions differ by far with respect to the psychiatric components specific to schizophrenia. Interestingly, it has recently been demonstrated that impaired ability to recognized emotions conveyed in auditory stimuli was related to poor disease outcome in schizophrenic patients, and related to impairments in a wide range of auditory functions [55].

4.3. Strengths and limitations

The superior temporal plane shows considerable individual variability. We cannot fully neglect a possible influence of interindividual variability on our results, despite spatial realignment. This may account for a certain amount of dispersion in spatial mapping, but we do not think that this would lead to primary regions merging with spatially remote secondary regions such as the STS, therefore our major observations hold.

To the best of our knowledge, the present dataset is the largest existing report of DES-induced auditory symptoms, providing a large spatial coverage of brain regions. Yet we cannot deny that this coverage remains sparse and is subject to a sampling bias. The ROI approach and the thresholding used – a minimum of 10 recordings per ROI, acknowledges and deals with this issue, at the cost of diminishing the very high spatial resolution of the raw SEEG data.

Finally, inherent to functional brain mapping based on intracortical exploration of focal drug-resistant epileptic patients is the risk of pathological brain states influencing the results, with the additional constraint that we needed the maximum available data for the probabilistic approach. The risk is mitigated at several levels. First, by including a large number of patients with anatomical anomalies widely distributed, the influence of pathology in a given region decreases. Second, by focusing on the time-window free of any epileptiform brain activity, during the stimulations, our probabilistic approach ensures that the brain signals targeted in the analysis are representative of physiological brain activity. Finally, we checked that the symptoms induced by DES targeted in the present study were not part of the patients' usual seizure experience. Thus, a trade-off was reached between using data from epileptic patients and deriving physiological information based on the maximum available data for the proposed probabilistic approach.

Data availability statement

The data can be made available upon request to the corresponding authors.

CRediT authorship contribution statement

Chloé Jaroszynski: contributed to data acquisition and analysis, contributed to drafting the manuscript and figures. **Ricardo Amorim-Leite:** contributed to data acquisition and analysis. **Pierre Deman:** contributed to data acquisition and analysis. **Marcela Perrone-Bertolotti:** contributed to data acquisition and analysis, contributed to drafting the manuscript and figures. **Florian Chabert:** contributed to data acquisition and analysis. **Anne-Sophie Job-Chapron:** contributed, to data acquisition and analysis. **Lorella Minotti:** contributed to data acquisition and analysis. **Dominique Hoffmann:** contributed to data acquisition and analysis. **Olivier David:** contributed to the conception and design of the study, contributed to data acquisition and analysis, contributed to drafting the manuscript and figures. **Philippe Kahane:** contributed to the conception and design of the study, contributed to data acquisition and analysis, contributed to drafting the manuscript and figures.

Declaration of competing interest

The authors declare that they have no known competing financial interests or personal relationships that could have appeared to influence the work reported in this paper.

Acknowledgements

The research leading to these results has received funding from the European Union's Horizon 2020 Framework Programme for Research and Innovation under Specific Grant Agreement No. 785907 and 945539 (Human Brain Project SGA2 and SGA3), from Grenoble-Alpes University Hospital grant (DRCI 1325, EPISTIM study), and from Agence Nationale pour la Recherche (International Collaborative Research Project ANR-DFG, RFTC project, ANR-18-CE92-0053-01).

Appendix A. Supplementary data

Supplementary data to this article can be found online at https://doi.org/10.1016/j.brs.2022.08.002.

References

[1] The American Association for Research into Nervous and Mental Diseases, Singer W. Consciousness and the structure of neuronal representations. Philos Trans R Soc Lond B Biol Sci 1998;353:1829–40.
[2] Badcock PB, Friston KJ, Ramstead MJD, Ploeger A, Hohwy J. The hierarchically mechanistic mind: an evolutionary systems theory of the human brain, cognition, and behavior. Cognit Affect Behav Neurosci 2019;19:1319–51.
[3] Barrett HC. A hierarchical model of the evolution of human brain specializations. Proc Natl Acad Sci USA 2012;109:10733–40.
[4] Chanes L, Barrett LF. Redefining the role of limbic areas in cortical processing. Trends Cognit Sci 2016;20:96–106.
[5] Elliott B, Joyce E, Shorvon S. Delusions, illusions and hallucinations in epilepsy: 1. Elementary phenomena. Epilepsy Res 2009;85:162–71.
[6] Chauvel P, McGonigal A. Emergence of semiology in epileptic seizures. Epilepsy Behav EB 2014;38:94–103.

[7] Hogan RE, Kaiboriboon K. The 'dreamy state': john Hughlings-Jackson's ideas of epilepsy and consciousness. Am J Psychiatr 2003;160:1740–7.
[8] Maillard L, et al. Semiologic and electrophysiologic correlations in temporal lobe seizure subtypes. Epilepsia 2004;45:1590–9.
[9] Florindo I, et al. Lateralizing value of the auditory aura in partial seizures. Epilepsia 2006;47:68–72.
[10] Penfield W, Kristiansen K. Seizure onset and the localization of epileptic discharge. Trans Am Neurol Assoc 1948;73:73–80.
[11] Catani M, Dell'Acqua F, Thiebaut de Schotten M. A revised limbic system model for memory, emotion and behaviour. Neurosci Biobehav Rev 2013;37:1724–37.
[12] Leaver AM, Seydell-Greenwald A, Rauschecker JP. Auditory-limbic interactions in chronic tinnitus: challenges for neuroimaging research. Hear Res 2016;334:49–57.
[13] Seydell-Greenwald A, Raven EP, Leaver AM, Turesky TK, Rauschecker JP. Diffusion imaging of auditory and auditory-limbic connectivity in tinnitus: preliminary evidence and methodological challenges. Neural Plast 2014;2014(1):43–59. https://doi.org/10.1155/2014/145943.
[14] Besteher B, et al. Chronic tinnitus and the limbic system: reappraising brain structural effects of distress and affective symptoms. NeuroImage Clin 2019;24:101976.
[15] Kapolowicz MR, Thompson LT. Plasticity in limbic regions at early time points in experimental models of tinnitus. Front Syst Neurosci 2020;13.
[16] Kahane P, et al. Electroclinical manifestations elicited by intracerebral electric stimulation 'shocks' in temporal lobe epilepsy. Neurophysiol Clin Clin Neurophysiol 1993;23:305–26.
[17] Kahane P. Epilepsy surgery in adult patients: for whom?. 160 Spec No 1 Rev Neurol (Paris) 2004;160(1):179–84.
[18] Kahane P, Spencer SS. Invasive evaluation. In: Handbook of clinical neurology, 108 vols. 867–879. Elsevier; 2012.
[19] Abel TJ, et al. Frameless robot-assisted stereoelectroencephalography in children: technical aspects and comparison with Talairach frame technique. J Neurosurg Pediatr 2018;22:37–46.
[20] Deman P, et al. IntrAnat electrodes: a free database and visualization software for intracranial electroencephalographic data processed for case and group studies. Front Neuroinf 2018;12:40.
[21] Zachlod D, et al. Four new cytoarchitectonic areas surrounding the primary and early auditory cortex in human brains. Cortex J Devoted Study Nerv Syst Behav 2020;128:1–21.
[22] Amunts K, Mohlberg H, Bludau S, Zilles K. Julich-Brain: a 3D probabilistic atlas of the human brain's cytoarchitecture. Science 2020;369:988–92.
[23] Gordon B, et al. Parameters for direct cortical electrical stimulation in the human: histopathologic confirmation. Electroencephalogr Clin Neurophysiol 1990;75:371–7.
[24] Tuyisenge V, et al. Automatic bad channel detection in intracranial electroencephalographic recordings using ensemble machine learning. Clin Neurophysiol 2018;129:548–54.
[25] David O, et al. Imaging the seizure onset zone with stereo-electroencephalography. Brain J Neurol 2011;134:2898–911.
[26] Perrone-Bertolotti M, et al. Probabilistic mapping of language networks from high frequency activity induced by direct electrical stimulation. Hum Brain Mapp 2020;41:4113–26.
[27] Grandchamp R, Delorme A. Single-trial normalization for event-related spectral decomposition reduces sensitivity to noisy trials. Front Psychol 2011;2:236.
[28] David O. Mapping of seizure networks. Oxford University Press. In: Invasive studies of the human epileptic brain, vols. 511–519; 2018. https://doi.org/10.1093/med/9780198714668.003.0038.
[29] Worsley KJ, Taylor JE, Tomaiuolo F, Lerch. J. Unified univariate and multivariate random field theory. Neuroimage 2004;23(Suppl 1):S189–95.
[30] Schreiber T, Schmitz A. Surrogate time series. Phys Nonlinear Phenom 2000;142:346–82.
[31] Halgren E, Chauvel P. Experimental phenomena evoked by human brain electrical stimulation. Adv Neurol 1993;63:123–40.
[32] Leaver AM, Rauschecker JP. Functional topography of human auditory cortex. J Neurosci 2016;36:1416–28.
[33] Allen EJ, Mesik J, Kay KN, Oxenham AJ. Dissociation of tonotopy and pitch in human auditory cortex. 2020.09.18.303651 bioRxiv 2020. https://doi.org/10.1101/2020.09.18.303651.
[34] Belin P, Zatorre RJ, Lafaille P, Ahad P, Pike B. Voice-selective areas in human auditory cortex. Nature 2000;403:309–12.
[35] Nourski KV. Auditory processing in the human cortex: an intracranial electrophysiology perspective. Laryngoscope Investig Otolaryngol 2017;2:147–56.
[36] Santoro R, et al. Encoding of natural sounds at multiple spectral and temporal resolutions in the human auditory cortex. PLoS Comput Biol 2014;10:e1003412.
[37] Glasser MF, et al. A multi-modal parcellation of human cerebral cortex. Nature 2016;536:171–8.
[38] Muller L, et al. Direct electrical stimulation of human cortex evokes high gamma activity that predicts conscious somatosensory perception. J Neural Eng 2018;15:026015.
[39] Rauschecker JP, Tian B. Mechanisms and streams for processing of 'what' and 'where' in auditory cortex. Proc Natl Acad Sci USA 2000;97:11800–6.
[40] Zatorre RJ, Bouffard M, Ahad P, Belin P. Where is 'where' in the human auditory cortex? Nat Neurosci 2002;5:905–9.
[41] Mullan S, Penfield W. Illusions of comparative interpretation and emotion; production by epileptic discharge and by electrical stimulation in the temporal cortex. AMA Arch Neurol Psychiatry 1959;81:269–84.
[42] Penfield W, Perot P. The Brain's record of auditory and visual experience. A final summary and discussion. Brain J Neurol 1963;86:595–696.
[43] Mulak A, Kahane P, Hoffmann D, Minotti L, Bonaz B. Brain mapping of digestive sensations elicited by cortical electrical stimulations. Neurogastroenterol Motil Off J Eur Gastrointest Motil Soc 2008;20:588–96.
[44] Bancaud J, Brunet-Bourgin F, Chauvel P, Halgren E. Anatomical origin of déjà vu and vivid 'memories' in human temporal lobe epilepsy. Brain J Neurol 1994;117(Pt1):71–90.
[45] Fish DR, Gloor P, Quesney FL, Olivier A. Clinical responses to electrical brain stimulation of the temporal and frontal lobes in patients with epilepsy. Pathophysiological implications. Brain J Neurol 1993;116(Pt 2):397–414.
[46] Halgren E, Walter RD, Cherlow DG, Crandall PH. Mental phenomena evoked by electrical stimulation of the human hippocampal formation and amygdala. Brain J Neurol 1978;101:83–117.
[47] Afif A, Hoffmann D, Minotti L, Benabid AL, Kahane P. Middle short gyrus of the insula implicated in pain processing. Pain 2008;138:546–55.
[48] Isnard J, Guénot M, Sindou M, Mauguière F. Clinical manifestations of insular lobe seizures: a stereo-electroencephalographic study. Epilepsia 2004;45:1079–90.
[49] Mazzola L, Isnard J, Peyron R, Guénot M, Mauguière F. Somatotopic organization of pain responses to direct electrical stimulation of the human insular cortex. Pain 2009;146:99–104.
[50] Morris HH, Lüders H, Lesser RP, Dinner DS, Hahn J. Transient neuropsychological abnormalities (including Gerstmann's syndrome) during cortical stimulation. Neurology 1984;34:877–83.
[51] Job A, et al. Specific activation of operculum 3 (OP3) brain region during provoked tinnitus-related phantom auditory perceptions in humans. Brain Struct Funct 2016;221:913–22.
[52] Job A, Jaroszynski C, Kavounoudias A, Jaillard A, Delon-Martin C. Functional connectivity in chronic nonbothersome tinnitus following acoustic trauma: a seed-based resting-state functional magnetic resonance imaging study. Brain Connect 2020;10:279–91.
[53] ffytche DH, Wible CG. From tones in tinnitus to sensed social interaction in schizophrenia: how understanding cortical organization can inform the study of hallucinations and psychosis. Schizophr Bull 2014;40:S305–16.
[54] Ćurčić-Blake B, et al. Interaction of language, auditory and memory brain networks in auditory verbal hallucinations. Prog Neurobiol 2017;148:1–20.
[55] Kraus MS, Walker TM, Jarskog LF, Millet RA, Keefe RSE. Basic auditory processing deficits and their association with auditory emotion recognition in schizophrenia. Schizophr Res 2019;204:155–61.